

# Deep Recurrent Electricity Theft Detection in AMI Networks with Random Tuning of Hyper-parameters

Mahmoud Nabil\*, Muhammad Ismail<sup>†</sup>, Mohamed Mahmoud\*, Mostafa Shahin<sup>†</sup>, Khalid Qaraqe<sup>†</sup>, and Erchin Serpedin<sup>†</sup>

\*Department of Electrical and Computer Engineering, Tennessee Tech. University, TN, USA

<sup>†</sup> Department of Electrical and Computer Engineering, Texas A&M University at Qatar, Doha, Qatar

**Abstract**—Modern smart grids rely on advanced metering infrastructure (AMI) networks for monitoring and billing purposes. However, such an approach suffers from electricity theft cyberattacks. Different from the existing research that utilizes shallow, static, and customer-specific-based electricity theft detectors, this paper proposes a generalized deep recurrent neural network (RNN)-based electricity theft detector that can effectively thwart these cyberattacks. The proposed model exploits the time series nature of the customers' electricity consumption to implement a gated recurrent unit (GRU)-RNN, hence, improving the detection performance. In addition, the proposed RNN-based detector adopts a random search analysis in its learning stage to appropriately fine-tune its hyper-parameters. Extensive test studies are carried out to investigate the detector's performance using publicly available real data of 107,200 energy consumption days from 200 customers. Simulation results demonstrate the superior performance of the proposed detector compared with state-of-the-art electricity theft detectors.

**Index Terms**—Electricity theft detection, cyberattacks, AMI networks, deep machine learning.

## I. INTRODUCTION

Electricity theft results in high financial losses for several countries such as the United States (\$6 billion/year) and India (\$17 billion/year) [1], [2]. Other developing countries lose almost 50% of their electricity revenue due to theft [3]. Recently, advanced metering infrastructure (AMI) networks are utilized within smart grids for monitoring, asset management, and billing purposes. The AMI networks rely on smart meters located in the customers' premises to regularly report their energy consumption. This approach has the potential to hinder traditional physical electricity theft attacks including line hooking or meter tampering [4]. Nevertheless, a new category of electricity theft attacks that target the AMI networks has appeared, namely electricity theft cyberattacks. These attacks jeopardize the integrity of the customer's energy consumption data as malicious customers hack into their smart meters to manipulate their own energy consumption values. Despite the difficulties associated with detecting such cyberattacks, the customers' fine-grained energy consumption data is considered to be a promising tool that can be used to boost automated electricity theft detection mechanisms.

Several automated theft detection techniques have been proposed in literature [5]–[17]. These detection techniques can be categorized into three main groups: machine learning, state estimation, and game theory-based techniques. Compared with

these techniques, machine learning-based techniques present the most mature and effective mechanism to tackle this problem due to their superior detection rate on real datasets [1]. However, the existing techniques suffer from several limitations. First, the existing detectors employ shallow machine learning architectures such as support vector machines (SVMs), while deep learning architectures can better capture the behavior of the input data resulting in a higher detection rate. In addition, the existing detectors rely on static input data [1], [13], however, exploiting the temporal correlation within the time series energy consumption data of the customers can further enhance the detection performance. Moreover, some of the existing works [1] adopt customer-specific models, where a detector's model is developed for each customer using only its energy consumption data in order to detect any future thefts. However, customer-specific models are not practical due to several reasons. On one hand, it would be impossible to train new detector models for new customers joining the system as these new customers do not have any historical energy consumption records. Furthermore, customer-specific detectors are not robust against contamination attacks, where the customer data that is used to train the detector is already malicious yet falsely labeled as honest data to confuse the detector.

In this work, our objective is to develop a generalized deep recurrent neural network (RNN)-based electricity theft detector. In specific, RNNs offer a considerable leverage while working with time series data since it is represented as a feedback network where the output at the current state is the input for the next state. To the best of our knowledge, only [14] investigates the application of deep neural networks for electricity theft detection. While a long-short-term-memory (LSTM) architecture of RNNs is investigated in [14] to tackle the electricity theft detection problem, a comprehensive study is needed to assess the performance of RNN-based detectors on real energy consumption data sets. In addition, further investigation should be considered in tuning the network hyper-parameters to further improve the training time and the model's performance.

The contributions of this paper are summarized as follows:

- We propose a generalized RNN-based electricity theft detector using hidden gated recurrent unit (GRU) layers. The generality of the model stems from its training on the energy consumption load profiles of different residential

customers' patterns.

- We carry out hyper-parameter tuning based on a random search to further improve the performance. Random search is proven to outperform grid search by finding a good hyper-parameter set in faster execution time [18].
- We evaluate the performance of the proposed detector using publicly available real data of 107,200 energy consumption days from 200 customers against a set of different types of cyber attacks. Simulation results demonstrate the robustness of the proposed model against existing detectors.

The remainder of this paper is organized as follows. Section II reviews the related work. Energy consumption data is presented in Section III. The proposed detection approach is explained in Section IV. Simulation results and discussions are presented in Section V. Finally, conclusions are drawn in Section VI.

## II. RELATED WORK

Several studies have addressed the problem of detecting electricity theft in the literature. Machine learning studies are the most pertinent to the proposed work. In [5], the authors compared the performance of two classification algorithms based on single feedforward neural network, namely, extreme learning machine (ELM), and online sequential extreme learning machine (OSELM), against SVM. The proposed approach was able to achieve 70% classification rate with ELM. Shallow SVM based detector has also been employed in [19] and achieved a detection accuracy up to 60% on real data set. The performance of this detector was further improved in [6] to reach an accuracy of 72% using a fuzzy inference system as a post-processing stage. A graph-based approach is proposed in [7] that uses optimum path forest for electricity theft detection and outperforms SVM with an accuracy of 89%. To the best of our knowledge, the best reported performance on a publicly available data set was achieved by [1], which employs an SVM classifier, with an average detection rate of 94% and a false acceptance rate of 11%.

Deep learning techniques for electricity theft detection are studied only in [14], where the author presents a comparison between different deep learning architectures such as convolutional neural networks (CNN), LSTM-RNNs, and stacked auto-encoders. Nevertheless, only two types of cyberattacks are presented and synthetic data is used to evaluate the performance of the proposed models, which cannot be compared reliably against models trained on real consumption data. Moreover, the effect of fine-tuning the models hyper-parameters is not studied in [14].

## III. ENERGY CONSUMPTION DATA

Define a set of customers  $\mathcal{C}$ , a set of days  $\mathcal{D} = \{1, \dots, D\}$ , and a set of periods  $\mathcal{T} = \{1, \dots, T\}$  of equal duration within each day. A smart meter is installed for each customer to regularly report the energy consumption for load monitoring and billing. For each customer  $c$ , the energy consumption value at a specific day  $d$  and time  $t$  is denoted as  $E_c(d, t)$ . Hence, each customer has an energy consumption record matrix  $E_c$  of

Table I  
CYBER ATTACKS IN [1].

Cyber Attack
$f_1(E_c(d, t)) = \alpha E_c(d, t)$
$f_2(E_c(d, t)) = \beta(d, t) E_c(d, t)$
$f_3(E_c(d, t)) = \begin{cases} 0 & \forall t \in [t_i(d), t_f(d)] \\ E_c(d, t) & \forall t \notin [t_i(d), t_f(d)] \end{cases}$
$f_4(E_c(d, t)) = \mathbb{E}[E_c(d)]$
$f_5(E_c(d, t)) = \beta(d, t) \mathbb{E}[E_c(d)]$
$f_6(E_c(d, t)) = E_c(d, T - t + 1)$

actual consumptions, where the rows of  $E_c$  span the days in  $\mathcal{D}$ , while the columns span the periods in  $\mathcal{T}$ . The smart meter reports the consumption to the utility for customer  $c$  on day  $d$  and period  $t$  as  $R_c(d, t)$ . An honest customer reports the actual energy consumed at the end of the consumption period, and hence,  $R_c(d, t) = E_c(d, t)$ . On contrary, a malicious customer aims to manipulate  $E_c(d, t)$  to lower its electricity bill by modifying the smart meter readings. Hence, the cyberattack is formally defined as  $R_c(d, t) = f(E_c(d, t))$ , where  $f(\cdot)$  denotes a cyberattack function that results in a reduced version for the malicious customer electricity bill. Although it is easy to collect honest samples for a customer  $c$  by monitoring its reports to the utility, malicious reports might not be easy to collect. This is because, the customer reports may all be honest or it has not been detected previously as a malicious customer. To tackle this problem, a set of cyberattack functions were defined in [1] as indicated in Table I. Each function  $f(\cdot)$  creates a different attack scenario that aims to reduce the customers' energy consumption  $E_c(d, t)$ . The first attack  $f_1(\cdot)$  aims to reduce  $E_c(d, t)$  by some fraction, where  $\alpha$  denotes a flat reduction percentage. On the other hand, attack  $f_2(\cdot)$  dynamically reduces  $E_c(d, t)$  by a value controlled by the time function  $\beta(d, t)$ . The third attack  $f_3(\cdot)$  represents a selective time filtering function, where the malicious customer reports zero reading during the interval  $[t_i(d), t_f(d)]$ , otherwise, the customer reports the actual consumption  $E_c(d, t)$ . Here,  $t_i(d)$  and  $t_f(d)$  denotes the initial and the final periods of the interval. The next two attacks  $f_4(\cdot)$  and  $f_5(\cdot)$  are based on the expected value of the energy consumption for the malicious customer for a given day denoted by  $\mathbb{E}[E_c(d)]$ . In  $f_4(\cdot)$ , the attacker reports a flat value during the day, while in  $f_5(\cdot)$  the attacker reduces  $\mathbb{E}[E_c(d)]$  dynamically from time to time using function  $\beta(d, t)$ . The last attack  $f_6(\cdot)$  is a reverse function that reorders the energy consumption reports during the day so that higher reports are assigned to low tariff periods.

Applying the aforementioned cyber attacks on the energy consumption record matrix  $E_c$  results in six matrices  $M_{c,i}$ , where  $i \in \{1, \dots, 6\}$ , for each attack  $f_i(\cdot)$ . The complete data set for a customer is denoted as  $\hat{X}_c$ , which is a concatenation for  $E_c$  and all malicious matrices  $M_{c,i}$ . In addition, each row  $X_c(d, \cdot)$  represents either an honest day sample (i.e.,  $E_c$  samples) labeled with 0 or a malicious sample (i.e.,  $M_{c,i}$

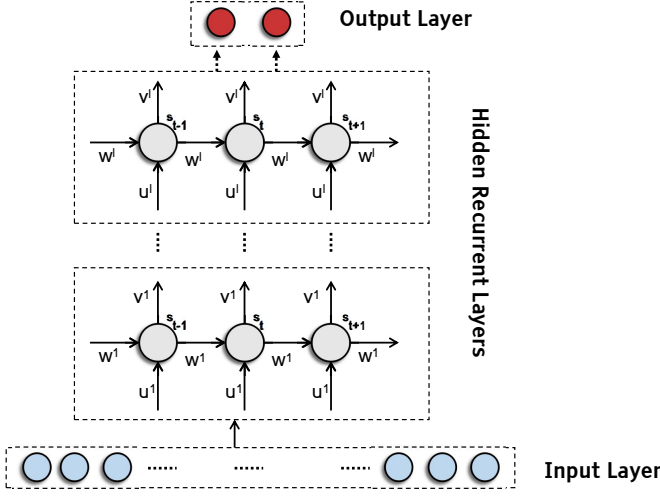


Figure 1. Architecture of general RNN-based electricity theft detector.

samples) labeled with 1. Since  $\hat{X}_c$  is an imbalanced dataset where the ratio of the honest samples to the malicious samples is 1:6, the detector may be biased towards the dominant class category (i.e., malicious samples). To mitigate the bias effect, the adaptive synthetic sampling approach (ADASYN) [20] is used to oversample the minor class so that the ratio between the honest and the malicious samples is almost the same. Each data set  $\hat{X}_c$  is partitioned into two disjoint data sets for model evaluation, specifically, a training set  $\hat{X}_{c,TR}$  and a testing set  $\hat{X}_{c,TST}$  with ratio 3:2. The training sets of all customers in  $\mathcal{C}$  are merged together to form  $\hat{X}_{TR}$ . Similarly, the test sets of all customers are merged together to form  $\hat{X}_{TST}$ . Hence, all customers have the same opportunity in training and evaluating the general model. As different customers have different ranges of energy consumption values during different report periods  $\mathcal{T}$ , different consumption periods have different opportunities to influence the optimization algorithm for the final model. Hence, in order to enforce equal opportunities for different consumption periods, feature scaling is applied to  $\hat{X}_{TR}$ . The mean and the variance of  $\hat{X}_{TR}$  are calculated and used to scale  $\hat{X}_{TR}$  so that each consumption period would have zero mean and unit standard deviation. The output of the feature scaling stage is denoted as  $X_{TR}$ . The same scaling scores are further applied to the test set to get  $X_{TST}$ .

To evaluate the performance of the detector, three metrics are used as follows. The detection rate (DR) measures the percentage of the correctly detected malicious attacks. The false acceptance (FA) rate measures the percentage of the honest samples that are falsely identified as malicious. The highest difference (HD) measures the difference between DR and FA [1]. The detection latency is ignored as electricity theft attacks do not result in an immediate loss to the utility. Moreover, malicious customers can be fined later for any detected thefts.

#### IV. DESIGN OF ELECTRICITY THEFT DETECTOR

This section describes the two stages used to develop the RNN-based general detector. The first is a training stage that

#### Algorithm 1: Electricity Theft Detector Training

---

**Data:**  $X_{TR}$   
**Result:** Optimal parameters  $U_{(\cdot)}^l, W_{(\cdot)}^l, V_{(\cdot)}^l$ , and  $b_{(\cdot)}^l$   
 $\forall l \in [1, \dots, L]$

- 1 **Initialization:** Weights  $U_{(\cdot)}^l, W_{(\cdot)}^l, V_{(\cdot)}^l$ , and  $b_{(\cdot)}^l$   
 $\forall l \in [1, \dots, L], i = 1$
- 2 **while**  $i \neq I$  **do**
- 3     Initialize:  $m = 1$
- 4     **while**  $m \neq M$  **do**
- 5         **for** each training example  $x$  in mini-batch  $m$  **do**
- 6             **Feed Forward:**
- 7             **for** each recurrent layer  $l$  **do**
- 8                 **for** each time step  $t$  **do**
- 9                      $z_t^l = \sigma(o_t^{l-1}U_z^l + s_{t-1}^lW_z^l + b_z^l)$
- 10                      $r_t^l = \sigma(o_t^{l-1}U_r^l + s_{t-1}^lW_r^l + b_r^l)$
- 11                      $h_t^l = \tanh(o_t^{l-1}U_h^l + (s_{t-1}^l \odot r_t^l)W_h^l + b_h^l)$
- 12                      $s_t^l = (1 - z_t^l) \odot h_t^l + z_t^l \odot s_{t-1}^l$
- 13                      $o_t^l = \text{softmax}(V^l s_t^l + b_o^l)$
- 14                 **end**
- 15             **end**
- 16             **Back propagation:** Compute  $\nabla_{U_{(\cdot)}^l} C(x)$ ,  
 $\nabla_{V_{(\cdot)}^l} C(x)$ ,  $\nabla_{W_{(\cdot)}^l} C(x)$ , and  $\nabla_{b_{(\cdot)}^l} C(x)$
- 17             **end**
- 18             **Weight and bias update:**
- 19              $U_{(\cdot)}^l = U_{(\cdot)}^l - \frac{\eta}{K} \sum_x \nabla_{U_{(\cdot)}^l} C(x)$
- 20              $V_{(\cdot)}^l = V_{(\cdot)}^l - \frac{\eta}{K} \sum_x \nabla_{V_{(\cdot)}^l} C(x)$
- 21              $W_{(\cdot)}^l = W_{(\cdot)}^l - \frac{\eta}{K} \sum_x \nabla_{W_{(\cdot)}^l} C(x)$
- 22              $b_{(\cdot)}^l = b_{(\cdot)}^l - \frac{\eta}{K} \sum_x \nabla_{b_{(\cdot)}^l} C(x)$
- 23             **end**
- 24         **end**
- 25     **end**

---

describes the detector architecture and parameters, and the second is the hyper-parameter optimization stage that uses a random search-based approach for fine-tuning.

##### A. Training Stage

The architecture of the RNN-based general detector is shown in Fig. 1. The input layer is denoted by vector  $x_c(d)$ , which represents the consumption vector of customer  $c$  during day  $d$  at different reporting periods  $t \in \mathcal{T}$ . The RNN architecture consists of  $L$  hidden GRU layers each with  $N$  neurons. Each GRU layer except the last one accepts a sequence vector as input and produces a sequence output vector. Unlike traditional feedforward layers, recurrent layers are more efficient in exploiting patterns from sequential information. The output layer has two neurons that define the malicious and the honest classes, where the true label can be represented by one-hot vector  $y(x_c(d)) = (0 \ 1)^T$  for honest customers, and  $y(x_c(d)) = (1 \ 0)^T$  for malicious customers.

The output vector from each layer  $l \in [1, \dots, L]$  is denoted as  $o^l$ , where  $o^1 = x(d)$ . Each hidden GRU layer  $l \in [2, \dots, L-1]$  has the following parameters:

---

**Algorithm 2: Random Search Hyper Parameters Optimization**


---

**Data:**  $X_{\text{TR}}$   
**Result:** Optimal hyper parameters  $L^*, N^*, O^*, A_H^*,$  and  $A_O^*$   
1 **Initialization:** Weights  $U_{(\cdot)}^l, W_{(\cdot)}^l, V_{(\cdot)}^l$ , and  $b_{(\cdot)}^l$   
 $\forall l \in [1, \dots, L], i = 1$   
2 **while**  $i \neq I$  **do**  
3    $L[i] \leftarrow \mathcal{L}, N[i] \leftarrow \mathcal{N}, O[i] \leftarrow \mathcal{O}, A_H[i] \leftarrow \mathcal{A}_H,$   
    $A_O[i] \leftarrow \mathcal{A}_O$   
4   **for** each  $\bar{X}_{\text{TR}}, \bar{X}_{\text{TST}}$  in  $k\text{-folds}(X_{\text{TR}})$  **do**  
5     Apply Algorithm 1 using sampled  
   hyper-parameters and record DR, FA and  
   accuracy.  
6   **end**  
7   Record average values across folds DR[i], FA[i] and  
   accuracy[i].  
8 **end**  
9 Report the hyperparameters of the top three models.

---

- The input at time step  $t$  is  $o_t^{l-1}$ , which results from the previous layer  $l-1$ .
- The hidden state  $s_t^l$  at time step  $t$  that represents the memory computed based on the previous hidden state  $s_{t-1}^l$  of the same layer.
- The update gate  $z_t^l = \sigma(o_t^{l-1}U_z^l + s_{t-1}^lW_z^l + b_z^l)$ , which determines a combination between the new input  $o_t^{l-1}$  and the previous memory  $s_{t-1}^l$ . Here,  $U_z^l$  and  $W_z^l$  are learnable weights,  $\sigma(\cdot)$  is the activation function, and  $b_z^l$  is the bias vector.
- The reset gate  $r_t^l = \sigma(o_t^{l-1}U_r^l + s_{t-1}^lW_r^l + b_r^l)$ , which determines the amount of the previous memory  $s_{t-1}^l$  that will contribute to the next state using the equation  $h_t^l = \tanh(o_t^{l-1}U_h^l + (s_{t-1}^l \odot r_t^l)W_h^l + b_h^l)$ . Here,  $U_r^l, W_r^l, U_h^l$ , and  $W_h^l$  are learnable weight matrices,  $b_r^l$  and  $b_h^l$  are the bias vectors, and  $\odot$  is the Hadamard product.
- The next state is simply  $s_{t+1}^l = (1 - z_t^l) \odot h_t^l + z_t^l \odot s_{t-1}^l$ , and the output at time  $t+1$  is  $o_{t+1}^l = \text{softmax}(V^l s_{t+1}^l + b_o^l)$ , where  $V^l$  is a learnable weight matrix.

The detector training stage involves learning the parameters  $U_{(\cdot)}^l, W_{(\cdot)}^l, V_{(\cdot)}^l$ , and  $b_{(\cdot)}^l$  for all layers, which results in the desired output vector  $y(x_c(d))$  for any input  $x_c(d)$ . The optimization objective to find these weights can be achieved by minimizing the cross-entropy cost function  $C$  defined as

$$\min_{\Theta} \frac{-1}{S} \sum_{X_{\text{TR}}} \{y^T(x_c(d)) \ln(o^L) + (1 - y^T(x_c(d))) \ln(1 - o^L)\}, \quad (1)$$

Where  $\Theta$  denotes the RNN parameters  $U_{(\cdot)}^l, W_{(\cdot)}^l, V_{(\cdot)}^l$ , and  $b_{(\cdot)}^l$  for all layers and  $S$  represents the total number of the training samples for all customers, which equals to the number of rows in  $X_{\text{TR}}$ . Solving (1) for the optimal parameters  $\Theta$  is done using an iterative gradient descent-based optimization algorithm. This is achieved by partitioning  $X_{\text{TR}}$  into  $M$  mini-batches of equal

size and executing Algorithm 1 for  $I$  total iterations. Each iteration  $i$  has two main stages, namely, feed forward and back-propagation. In the feed forward stage, the training samples in the mini-batch are passed through all the network layers to calculate the predicted output vectors. On the other hand, the back propagation stage uses the mini-batches to calculate the gradient of the cost function in (1) with respect to the network weights [21]. Thereafter, the computed gradients are used to modify the weights and biases for each iteration. Note that, the back propagation within each layer is basically a back propagation through time (BPTT) as each layer is a GRU. In addition,  $\nabla_a$  in Algorithm 1 denotes the partial derivative with respect to  $a$ . Algorithm 1 uses stochastic gradient descent (SGD) for optimization with learning rate  $\eta$ .

### B. Hyper-parameters Optimization Stage

Tuning the hyper-parameters of the detector is a challenging and a time-consuming task, however, optimal parameters improve the detector performance. Since an exhaustive search on hyper-parameters is practically infeasible due to the incurred high computational complexity, random search is used to find a sub-optimal but an efficient solution in a reduced time compared with the exhaustive grid search [18]. In this paper, random search is used to tune the following hyper-parameters: the network architecture in terms of the number of hidden layers and the number of neurons within each hidden layer, the type of activation functions used at the RNN layers, the type of activation functions used at the output layer, and the type of gradient descent-based optimization algorithm used in finding the optimal RNN parameters (weights and biases) [21]. Denote  $\mathcal{L}$  and  $\mathcal{N}$  as two uniform distributions that represent the number of hidden layers and neurons to be sampled by the random search algorithm. In addition, Let  $\mathcal{O}$  represent a uniform distribution of optimization algorithms that can include Adam, SGD, Adamax, etc. [21]. Moreover, two uniform distributions are defined to represent the set of activation functions used by the hidden and output layers, namely,  $\mathcal{A}_H$  and  $\mathcal{A}_O$ , respectively. Algorithm 2 shows the random search over  $X_{\text{TR}}$  for the selection of the optimal hyper-parameters defined as  $P^*$ . The maximum number of search iterations is denoted as  $I$ , where at each iteration all the distributions are sampled uniformly and the sampled model is evaluated using K-fold cross-validation.

## V. NUMERICAL RESULTS AND DISCUSSION

To evaluate the performance of the proposed RNN-based general electricity theft detector, real smart meter data from the Irish Smart Energy Trials is used [22]. The data set was published by the Electric Ireland and Sustainable Energy Authority of Ireland in January 2012. It contains the energy consumption readings for 5000 customers over 536 days between 2009 – 2010. The customers report their readings every 30 minutes (i.e., the RNN input size is 48), and hence, the total number of reports per customer is 25,728. Daily reports from 200 customers with 107,200 days are considered as honest energy consumption records, which are then used to launch the

Table II  
SAMPLED HYPER-PARAMETERS RESULTS OF ALGORITHM 2 USING K-FOLD CROSS VALIDATION.

$L$	$N$	$\mathcal{A}_H$	$\mathcal{A}_O$	$\mathcal{O}$	DR	FA	HD	Accuracy
2	201	Hard Sigmoid	Sigmoid	Adam	0.930	0.029	0.900	0.950
	384	Sigmoid	Sigmoid	SGD	0.707	0.313	0.394	0.697
	<b>428</b>	<b>Sigmoid</b>	<b>Softmax</b>	<b>Adamax</b>	<b>0.946</b>	<b>0.036</b>	<b>0.910</b>	<b>0.955</b>
	270	Relu	Sigmoid	Nadam	0	0	0	0.499
	306	Hard Sigmoid	Softmax	SGD	0.727	0.324	0.403	0.701
	258	Hard Sigmoid	Sigmoid	SGD	0.713	0.311	0.402	0.701
	154	Hard Sigmoid	Softmax	Adagrad	0.880	0.067	0.812	0.906
	250	Tanh	Sigmoid	Adadelata	0.916	0.051	0.865	0.932
	351	Sigmoid	Softmax	Adamax	0.941	0.035	0.905	0.952
	284	Hard Sigmoid	Softmax	SGD	0.739	0.340	0.398	0.699
3	105	Tanh	Sigmoid	Adagrad	0.877	0.083	0.793	0.896
	385	Tanh	Sigmoid	Adadelata	0.928	0.037	0.890	0.945
	307	Sigmoid	Sigmoid	RMSprop	0.923	0.031	0.891	0.945
	239	Tanh	Sigmoid	Adagrad	0.609	0.328	0.281	0.640
	272	Hard Sigmoid	Sigmoid	Adadelata	0.885	0.071	0.813	0.906
	110	Sigmoid	Softmax	Nadam	0.928	0.036	0.891	0.945
	251	Tanh	Sigmoid	Nadam	0	0	0	0.499
	<b>310</b>	<b>Hard Sigmoid</b>	<b>Softmax</b>	<b>Adam</b>	<b>0.939</b>	<b>0.033</b>	<b>0.905</b>	<b>0.952</b>
	407	Hard Sigmoid	Sigmoid	Adagrad	0.867	0.075	0.791	0.895
	193	Sigmoid	Sigmoid	Adadelata	0.875	0.068	0.807	0.903
4	492	Relu	Sigmoid	SGD	0	0	0	0.499
	198	Tanh	Softmax	RMSprop	0.419	0.186	0.232	0.615
	352	Sigmoid	Softmax	Adamax	0.931	0.026	0.905	0.952
	<b>215</b>	<b>Tanh</b>	<b>Softmax</b>	<b>Adamax</b>	<b>0.942</b>	<b>0.028</b>	<b>0.914</b>	<b>0.957</b>
	275	Tanh	Softmax	Adam	0	0	0	0.499
	202	Relu	Sigmoid	Adagrad	0	0	0	0.499
	393	Sigmoid	Sigmoid	RMSprop	0.939	0.044	0.894	0.947
	165	Sigmoid	Softmax	Adagrad	0.898	0.073	0.825	0.912
	390	Hard Sigmoid	Sigmoid	Adadelata	0.608	0.359	0.249	0.624
	310	Tanh	Sigmoid	RMSprop	0.187	0.126	0.061	0.530

cyberattacks given in Table I for each customer. For cyberattacks  $f_1(\cdot)$ ,  $f_2(\cdot)$ , and  $f_5(\cdot)$ ,  $\alpha$  and  $\beta(d, t)$  are random variables that are uniformly distributed over the interval  $[0.1, 0.8]$  [1]. For attack  $f_3(\cdot)$ ,  $t_i(d)$  is a uniform random variable in  $[0, 42]$ , and the duration of the attack, i.e.,  $t_f(d) - t_i(d)$ , is a uniform random variable in  $[8, 48]$ , and hence, the maximum value of  $t_f(d) = 48$ . Applying all cyberattacks for each customer results in  $\hat{X}_c$  data set which contains 536 honest samples (days) and 3,216 malicious samples. Each sample in  $\hat{X}_c$  has 48 energy consumption values. For each  $\hat{X}_c$  data set, over-sampling is performed to balance the size of honest and malicious classes. Consequently, the total size of each  $\hat{X}_c$  data set contains a total of 6,432 honest and malicious samples. The total number of samples for all  $c \in \mathcal{C}$  is 1,286,400. Each  $\hat{X}_c$  data set is partitioned into training set  $\hat{X}_{c, \text{TR}}$  and testing set  $\hat{X}_{c, \text{TST}}$  with ratio 3:2. The training sets for all customers are merged together to form  $\hat{X}_{\text{TR}}$ . Similarly, the test sets for all customers are merged together to form  $\hat{X}_{\text{TST}}$ . Feature scaling on training data produces  $X_{\text{TR}}$  and applying the same scores on the test data produces  $X_{\text{TST}}$ .

In Algorithm 1, the total number of epochs  $I = 10$  and the batch size is 350. For Algorithm 2, the options used for the random search are the following:  $\mathcal{L} = \{2, 3, 4\}$ ,  $\mathcal{N} = [100, 500]$ ,  $\mathcal{O} = \{\text{SGD}, \text{Adadelata}, \text{Adagrad}, \text{Adam}, \text{Adamax},$

$\text{Nadam}, \text{RMSprop}\}$ ,  $\mathcal{A}_H = \{\text{Sigmoid}, \text{Relu}, \text{Hard Sigmoid}, \text{Tanh}\}$ , and  $\mathcal{A}_O = \{\text{Sigmoid}, \text{Softmax}\}$ . In addition, the total number of iterations is  $I = 30$ , the drop out rate is set to 0.2 and the initialization of the network neurons is set to Glorot Uniform [21]. All the experiments were performed on the high-performance cluster (HPC) of the Tennessee Tech University using two NVIDIA Tesla K80 GPUs. Tensorflow and Python Keras Library are used for the implementation.

Table II gives the random search evaluation results obtained by applying Algorithm 2 on the sampled hyper-parameters. The results give the average detection performance over K-fold cross-validation (with  $K = 3$ ) on  $X_{\text{TR}}$  in terms of DR, FA, and HD. As indicated in the table, the proposed general electricity theft detector benefits from the recurrent deep architecture as the HD can achieve 91.4%. It can also be noticed that all the networks that have Relu samples failed to optimize properly, which is attributed to the finding discussed in [23] in which deep sigmoidal networks can outperform deep Relu networks if initialized properly. Moreover, all the networks with SGD optimizer struggle to achieve good results, which can be attributed to the small number of epochs used for the training. Finally, all the promising models have Softmax activation for the output layer. The top three models with respect to HD for each number of layers  $l \in \{2, 3, 4\}$  are highlighted in Table II

Table III  
AVERAGE PERFORMANCE OF THE THEFT DETECTOR.

	MD1	MD2	MD3	[1]
DR (%)	<b>93.4</b>	92.5	92.7	94
FA (%)	6.9	<b>5.0</b>	5.3	11
HD (%)	86.4	<b>87.4</b>	87.4	83

and further used for performance evaluation using the test set  $X_{TST}$ .

Table III gives a comparison between the top three models highlighted in Table II and the model proposed in [1], which was tested by the same data used in this paper. The first three columns in Table III give the average performance results when using the best hyper-parameters highlighted in Table II, such that the models with  $l = 2$ ,  $l = 3$ , and  $l = 4$  are represented by MD1, MD2, and MD3, respectively. The last column gives the results from [1]. While the detector in [1] is trained on the same dataset used in this paper, it is a customer-specific electricity theft detector based on a shallow machine learning architecture (SVM). As indicated in Table II, the best HD is achieved when MD2 or MD3 hyper-parameters are applied, which outperforms the proposed detector in [1] by a 4% increase. Moreover, the FA is improved by almost 55%. The results indicate that an improvement in the electricity theft detection performance can be achieved using RNN architecture. In addition, our proposed detector is a general model that does not rely on a specific customer data. Hence, it is more robust against contamination attacks compared with the proposed detector in [1].

## VI. CONCLUSION

A general RNN-based electricity theft detector is proposed. The proposed detector exploits the time series nature of the customers' energy consumption to implement GRU deep hidden layers that can learn complex patterns of customers' consumption yielding better detection performance. Random search is employed to tune the detector hyper-parameters and further improve the performance. Load profiles comprising 107,200 days for different customers over two years are the basis for the experiments. The proposed RNN-based detector achieves a detection rate up to 93% and a false acceptance rate as low as 5%, which presents a 55% reduction in false acceptance, and 4% improvement in the highest difference rate compared with a benchmark detector in the literature. Moreover, the proposed detector is more robust against contamination attacks as it does not rely on a specific customer data.

## VII. ACKNOWLEDGMENT

This publication was made possible by NPRP grant # NPRP9-055-2-022 from the Qatar National Research Fund (a member of Qatar Foundation). The statements made herein are solely the responsibility of the authors.

## REFERENCES

[1] P. Jokar, N. Arianpoo, and V. C. Leung, "Electricity theft detection in AMI using customers' consumption patterns," *IEEE Transactions on Smart Grid*, vol. 7, no. 1, pp. 216–226, 2016.

[2] S. K. Singh, R. Bose, and A. Joshi, "Entropy-based electricity theft detection in AMI network," *IET Cyber-Physical Systems: Theory & Applications*, 2017.

[3] P. Antmann, "Reducing technical and non-technical losses in the power sector," *World Bank, Washington, DC*, 2009.

[4] P. Pickering, "E-Meters Offer Multiple Ways to Combat Electricity Theft and Tampering," Last accessed: Nov 2017. [Online]. Available: <http://www.electronicdesign.com/meters/e-meters-offer-multiple-ways-combat-electricity-theft-and-tampering>

[5] A. Nizar, Z. Dong, and Y. Wang, "Power utility nontechnical loss analysis with extreme learning machine method," *IEEE Transactions on Power Systems*, vol. 23, no. 3, pp. 946–955, 2008.

[6] J. Nagi, K. S. Yap, S. K. Tiong, S. K. Ahmed, and F. Nagi, "Improving SVM-based nontechnical loss detection in power utility using the fuzzy inference system," *IEEE Transactions on power delivery*, vol. 26, no. 2, pp. 1284–1285, 2011.

[7] C. Ramos, A. de Sousa, J. Papa, and X. Falcao, "A new approach for nontechnical losses detection based on optimum-path forest," *IEEE Transactions on Power Systems*, vol. 26, no. 1, pp. 181–189, 2011.

[8] E. Angelos, O. Saavedra, C. Cortés, and A. de Souza, "Detection and identification of abnormalities in customer consumptions in power distribution systems," *IEEE Transactions on Power Delivery*, vol. 26, no. 4, pp. 2436–2442, 2011.

[9] C.-H. Lin, S.-J. Chen, C.-L. Kuo, and J.-L. Chen, "Non-cooperative game model applied to an advanced metering infrastructure for non-technical loss screening in micro-distribution systems," *IEEE Transactions on Smart Grid*, vol. 5, no. 5, pp. 2468–2469, 2014.

[10] S. Amin, G. A. Schwartz, A. A. Cardenas, and S. S. Sastry, "Game-theoretic models of electricity theft detection in smart utility networks: Providing new capabilities with advanced metering infrastructure," *IEEE Control Systems*, vol. 35, no. 1, pp. 66–81, 2015.

[11] Y. Zhou, X. Chen, A. Y. Zomaya, L. Wang, and S. Hu, "A dynamic programming algorithm for leveraging probabilistic detection of energy theft in smart home," *IEEE Transactions on Emerging Topics in Computing*, vol. 3, no. 4, pp. 502–513, 2015.

[12] Y. Liu and S. Hu, "Cyberthreat analysis and detection for energy theft in social networking of smart homes," *IEEE Transactions on Computational Social Systems*, vol. 2, no. 4, pp. 148–158, 2015.

[13] A. Jindal, A. Dua, K. Kaur, M. Singh, N. Kumar, and S. Mishra, "Decision tree and SVM-based data analytics for theft detection in smart grid," *IEEE Transactions on Industrial Informatics*, vol. 12, no. 3, pp. 1005–1016, 2016.

[14] R. R. Bhat, R. D. Trevizan, R. Sengupta, X. Li, and A. Bretas, "Identifying nontechnical power loss via spatial and temporal deep learning," in *Proc. of 15th IEEE International Conference on Machine Learning and Applications (ICMLA)*, 2016, pp. 272–279.

[15] T.-S. Zhan, S.-J. Chen, C.-C. Kao, C.-L. Kuo, J.-L. Chen, and C.-H. Lin, "Non-technical loss and power blackout detection under advanced metering infrastructure using a cooperative game based inference mechanism," *IET Generation, Transmission & Distribution*, vol. 10, no. 4, pp. 873–882, 2016.

[16] M. Tariq and H. V. Poor, "Electricity theft detection and localization in grid-tied microgrids," *IEEE Transactions on Smart Grid*, 2016.

[17] F. Xiao and Q. Ai, "Electricity theft detection in smart grid using random matrix theory," *IET Generation, Transmission & Distribution*, 2017.

[18] J. Bergstra and Y. Bengio, "Random search for hyper-parameter optimization," *Journal of Machine Learning Research*, vol. 13, no. Feb, pp. 281–305, 2012.

[19] J. Nagi, K. S. Yap, S. K. Tiong, S. K. Ahmed, and M. Mohamad, "Nontechnical loss detection for metered customers in power utility using support vector machines," *IEEE transactions on Power Delivery*, vol. 25, no. 2, pp. 1162–1171, 2010.

[20] H. He, Y. Bai, E. A. Garcia, and S. Li, "Adasyn: Adaptive synthetic sampling approach for imbalanced learning," in *Proc. of IEEE International Joint Conference on Computational Intelligence*, 2008, pp. 1322–1328.

[21] I. Goodfellow, Y. Bengio, and A. Courville, *Deep learning*. MIT press, 2016.

[22] "Irish Social Science Data Archive," Last accessed: Nov 2017. [Online]. Available: <http://www.ucd.ie/issda/data/commissionforenergyregulationcer/>

[23] J. Pennington, S. Schoenholz, and S. Ganguli, "Resurrecting the sigmoid in deep learning through dynamical isometry: theory and practice," in *Advances in neural information processing systems*, 2017, pp. 4788–4798.